MRS Advances © 2016 Materials Research Society
DOI: 10.1557/adv.2016.149

Fabrication of an Electrochemical Sensor for Glucose Detection using ZnO Nanorods

Sanghamitra Mandal[1], Mohammed Marie[2] and Omar Manasreh[1]
[1] Department of Electrical Engineering, University of Arkansas, Fayetteville, AR 72701, U.S.A.
[2] Microelectronics Photonics Program, University of Arkansas, Fayetteville, AR 72701, U.S.A.

ABSTRACT

An electrochemical glucose sensor based on zinc oxide (ZnO) nanorods is fabricated, characterized and tested. The ZnO nanorods are synthesized on indium titanium oxide (ITO) coated glass substrate, using the hydrothermal sol-gel technique. The working principle of the sensor under investigation is based on the electrochemical reaction taking place between cathode and anode, in the presence of an electrolyte. A platinum plate, used as the cathode and Nafion/Glucose Oxidase/ZnO nanorods/ITO-coated glass substrate used as anode, is immersed in pH 7.0 phosphate buffer solution electrolyte to test for the presence of glucose. Several amperometric tests are performed on the fabricated sensor to determine the response time, sensitivity and limit of detection of the sensor. A fast response time less than 3 s with a high sensitivity of 1.151 mA $cm^{-2}mM^{-1}$ and low limit of detection of 0.089 mM is reported. The glucose sensor is characterized using the cyclic voltammetry method in the range from -0.8 – 0.8 V with a voltage scan rate of 100 mV/s.

INTRODUCTION

Today, health issues caused by diabetes have affected 350 million people in the world, causing high rates of illness and deaths [1]. Glucose is the most important form of sugar in the human blood that acts as the prime source of energy for the human body. Monitoring normal blood glucose level prevents the risks of suffering from the chronic disease diabetes. It is reported that zinc oxide (ZnO) nanowires are biodegradable and biocompatible in bio fluids [2]. The isoelectric point of ZnO is 9.5 that makes nanostructured ZnO materials to easily absorb enzymes in buffer solutions [3]. The stability of ZnO in air is high [4]. The oxide layers naturally formed on zinc do not form a passivating film, which prevents its corrosion [5]. In the recent years, one dimensional ZnO nanorods are synthesized using the hydrothermal growth technique [6]. In this paper, an enzyme based amperometric electrochemical glucose sensor is reported. In such sensors, high rate of enzyme mobilization with an appropriate transducer material is desired [7]. The working of amperometric sensors are based on the detection of hydrogen peroxide (H_2O_2) during the enzymatic reaction by anodic oxidation [8]. Platinum is one of the most commonly used transducer electrodes used in amperometric sensors [8]. A sensitivity of 1151 μA/cm2 mM is reported for the investigated Nafion/GOx/ZnO NRs/ITO coated glass substrate electrode. The sensitivity is derived from the linear response slope obtained for a glucose concentration ranging from 0.01 – 1.6 mM. The acquired sensitivity slope is extremely high compared to peer results reported on glucose sensors based on ZnO nanocombs [11], ZnO nanorods arrays [10, 12], ZnO nanotubes [9, 13], ZnO nanowires [14] and ZnO inverse opal [14] (See Appendix: Table I). Also, the limit of detection varies between 0.001 – 0.070 mM [9, 10-17] as compared to 0.089 mM reported in this paper. In this paper, a response time less than 3 s is reported that is faster considering previous papers reported on enzymatic glucose sensors based on different nanomaterials like titanium sol-gel membrane [15], carbon

decorated ZnO nanowires on titanium [16], and nanostructured cerium oxide film [17] (See Appendix: Table I).

EXPERIMENT

All the chemicals used during the experiment were purchased from VWR International or Sigma-Aldrich without further purification. A 0.5M ZnO sol-gel is prepared by stirring 1.1 g of zinc acetate in 10 mL of mono-ethanolamine for 1 hour at a temperature of 70 $^{\circ}$C. A milky dull solution is formed to which 0.3 mL of ethanolamine is added and stirred for an hour at 70 $^{\circ}$C. The ZnO sol-gel is spin-coated on indium titanium oxide (ITO) coated glass substrate to form a thin-film over the substrate surface. A 0.05 M ZnO nanorods growth solution is prepared by stirring 0.3 g of zinc nitrate hexa-hydrate, and 0.14 g of hexamethylenetetramine, respectively in 10 mL of de-ionized water at room temperature for an hour. The ITO substrate coated with thin film is immersed into the growth solution upside down at a temperature of 85 $^{\circ}$C for 4 hours. The sample is then, rinsed with deionized water and annealed at room temperature for 30 min at a temperature of 110 $^{\circ}$C.

The sample with well-aligned hexagonal ZnO nanorods is characterized using absorbance, Raman and scanning electron microscopies, and Gonio mode X-ray diffraction (XRD) using Cary 500 Scan UV-Vis-NIR spectrophotometer, Horiba LabRAM HR Raman spectroscope, scanning electron microscope, and Philips PW 1830 double system diffractometer, respectively. Sensor fabrication is performed using an enzyme that is prepared by sonicating 40 mg Bovine serum albumin and 20 mg glucose oxidase (GOx) in 0.4 mL phosphate buffer solution (PBS). The polymer nafion (0.2µL) is dropped on the sample to stabilize the GOx and prevent enzyme leakage. The sample with Nafion/GOx/ZnO nanorods/ITO-coated glass substrate, and platinum plate are, respectively used as anode and cathode, to measure current response for a constant voltage of 0.8 V by means of the Keithley 2410 source meter. Redox state studies are performed using cyclic voltammetry for a voltage range from -0.8 V – 0.8 V with a voltage sweep rate of 100 mV/s.

DISCUSSION

The ultraviolet - visible absorbance spectroscopy is measured at room temperature for the hydrothermal ZnO nanorods grown for a wavelength ranging from 200 nm to 1000 nm. A prominent exciton band peak is observed at 365 nm as depicted in Fig. 1. A blue shift is witnessed when compared to the absorbance of bulk ZnO at 374 nm [18]. The particle size of ZnO nanorods with radius 1.1 + 0.1 nm slightly decreases when compared to the bulk ZnO exciton Bohr's radius ~ 2.34 nm [19]. The band gap expansion and blue shift in the absorbance spectrum occurs due to quantum confinement in the ZnO nanorods [19] synthesized using the sol-gel growth method. Raman spectroscopy is utilized to determine the lattice distortions in ZnO nanorods caused by oxygen vacancies and impurities. The Raman spectrum shown in Fig. 2 has dominant peaks at 332, 380, 439.7, and 584 cm^{-1}. These peaks are called the E_2 low second order Raman mode, A_1 transverse optical mode, non-polar E_2 high optical phonon mode, and the E_1 longitudinal optical mode, respectively. The location of the modes is determined by the crystal orientation, and polarization of the incident and Raman scattered lights [20].

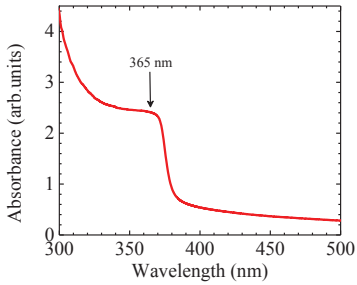

Figure 1. Absorbance spectrum of hydrothermally grown ZnO nanorods measured at room temperature.

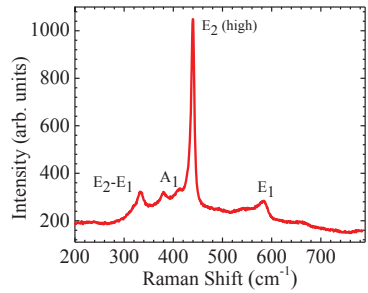

Figure 2. Micro-Raman spectrum for ZnO nanorods grown on ITO coated glass substrate after hot plate annealing at 120°C.

The top view scanning electron microscopy (SEM) image of the sample substrate with ZnO nanorods is represented in Fig. 3. The nanorods are hexagonal in shape, well-aligned and evenly distributed throughout the surface of the ITO-coated glass substrate. The length and diameter of the ZnO nanorods is ~ 1.5 µm and ~ 70 nm, respectively. The aspect ratio is calculated as 21. Aspect ratio is referred to as the ratio of the average length to the average width of the nanorods. The crystal structure and orientation of the ZnO nanorods are studied using the Gonio-mode XRD pattern as shown in Fig. 4. The most dominant peak appears at 34.364° representing the (002) orientation of the ZnO 2Theta scan XRD pattern. Other peaks at 36.208°, 47.469°, 62.756°, and 72.429°, denote the (101), (102), (103), and (004) orientation XRD peaks of ZnO. The lattice constants calculated using the (002) orientation is a = 3.0111 Å and c = 5.2153 Å, which are in good agreement with the bulk ZnO [21]. The Scherrer's equation $\tau = \frac{K \cdot \lambda}{\beta \cdot \cos\theta}$ [22] is used to determine the average crystal size (~ 7.64 Å) for (002) orientation ZnO. In the above equation, K, λ, β, and θ are shape factor (0.9), the X-ray wavelength (1.5406 Å), FWHM (0.19°), and Bragg's diffraction angle (17.182°), respectively.

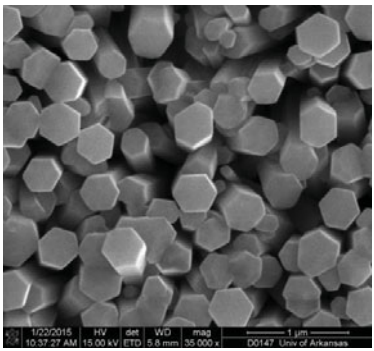

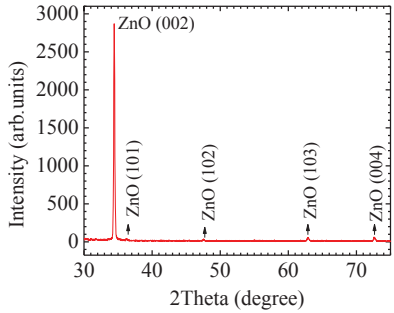

Figure 3. SEM image of ZnO nanorods grown using the sol-gel hydrothermal method on ITO and measured at room temperature.

Figure 4. Gonio-XRD pattern of ZnO nanorods at room temperature.

The sketch of the working electrode Nafion/GOx/ZnO nanorods/ITO-coated glass substrate is shown in Fig. 5 (a). The substrate with ZnO nanorods are rinsed with PBS to create a hydrophilic surface. 1 µL of GOx is dropped onto ZnO nanorods at room temperature and allowed to dry for a couple of hours. 2 µL Nafion polymer is dropped onto the substrate with GOx adsorbed ZnO nanorods and dried in air for a couple of hours. Nafion is highly permeable in water and is capable of resisting chemical attack. The ion exchanging properties of nafion creates a biocompatible layer for the enzymes and stabilizes GOx. Figure 5 (b) illustrates the schematic for the glucose sensing electrochemical experiment setup. The working electrode Nafion/GOx/ZnO nanorods/ITO acts as the anode, and a platinum plate as the cathode that are immersed into the pH 7.0 electrolyte PBS. A potential of 0.8 V is applied across the two electrodes to record the current responses of the sensor.

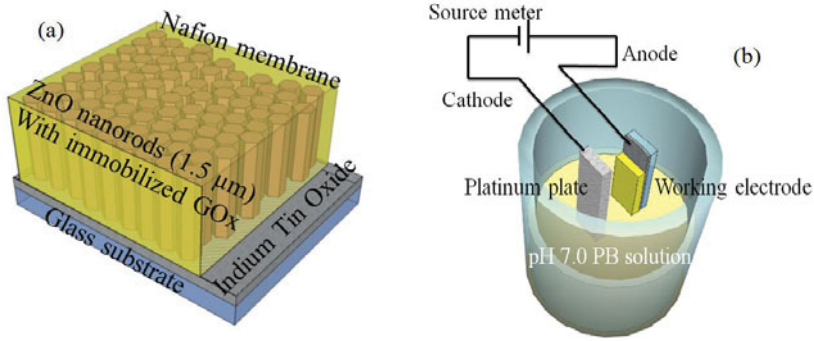

Figure 5. (a) Nafion/GOx/ZnO nanorods/ITO electrode. **(b)** Schematic illustration of the electrochemical test cell with anode and cathode immersed in PBS.

The current response for different concentrations of glucose in PBS is recorded to obtain the calibration curve shown in Fig. 6. The calibration curve is achieved utilizing the steady-state amperometric response for increasing glucose concentrations, added to the pH 7.0 PBS inside the test cell. Steady-state amperometric response refers to the current versus time response. The error bars represent 4% standard deviation for 10 consecutive amperometric responses. During the phenomenon of electrolysis inside the test cell at 0.8 V, glucose gets oxidized by GOx to produce an enzyme. Reaction of this enzyme with oxygen produces H_2O_2. Reduction of H_2O_2 chemically occurs as: $H_2O_2 \rightarrow O_2 + 2H + 2e^-$. The electrons given out into the electrolyte during the electrochemical reaction gives the sensor sensitivity. Based on the amperometric measurements, response time of the sensor is calculated to be $\leq$ 3 s, which is faster than the sensors reported earlier with an aspect ratio of 30 [10]. The slope and the intercept of the curve in Fig. 6 exhibits a sensitivity of 1.151 mA/cm^2 mM, for a linear range of increasing glucose concentration ranging from 0.01 – 1.6 mM, measured at a fixed potential of 0.8 V. The sensitivity achieved is high compared to peer reviewed results reported on glucose sensors based on ZnO nanorods arrays [10, 12]. Limit of detection (LOD) is the minimum amount of glucose

analyte concentration in PBS that is distinguished from zero [23]. Thus, LOD = $\frac{3 \times \text{Standard deviation}}{\text{Slope}}$ [24], where the y-intercept of the linear fit is considered as the standard deviation. The LOD is calculated as 0.089 mM. The normal glucose level in humans, fall in between the range from 3.5 – 6.1 mM, whereas in case of a diabetic person it could be as high as 18 mM [14]. This clinical glucose range justifies the detection range, and achieved LOD reported in this paper. The cyclic voltammogram presented in Fig. 7 has a reduction peak at -0.45 V indicating reduction of H_2O_2, and an oxidation peak at 0.45 V demonstrating the oxidation of glucose. It can be inferred that with the increase in the glucose concentration successively added to PBS leads to an increase in the rate of glucose oxidation by enzyme GOx that are seen as the redox peaks in the voltammogram (Fig. 7).

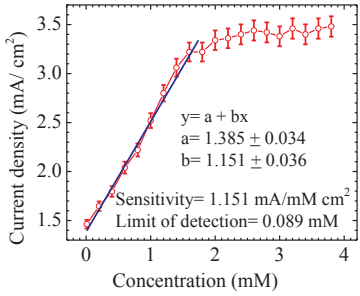

Figure 6. Calibration curve plotted using the amperometric response measured at a potential of 0.8 V, for glucose concentration ranging from 0.01 – 20 mM.

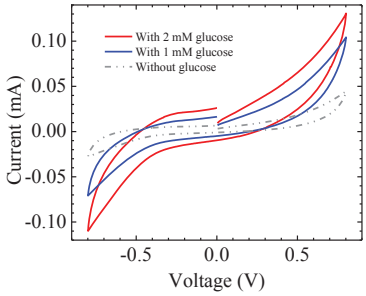

Figure 7. Cyclic-voltammogram of electrochemical glucose sensor for a potential ranging from -0.8 V – 0.8 V with a sweep rate of 100 mV/sec

CONCLUSIONS

An enzymatic electrochemical glucose sensor based on the phenomenon of GOx adsorption by hydrothermally grown ZnO nanorods is reported. The high isoelectric point of ZnO aids in easy absorption of enzymes, whereas its stability in air, and biocompatibility creates an atmosphere for retaining enzyme activity. A simple and low-temperature method known as the hydrothermal sol-gel technique is used to synthesize ZnO nanorods with high aspect ratio. The immobilization efficiency of GOx being absorbed by the ZnO nanorods depends upon the aspect ratio of the nanorods. The hydrothermal synthesis growth conditions control the surface morphology and distribution of the ZnO nanorods, grown on the desired substrate. High aspect ratio ZnO nanorods are utilized to improve the electrical contact for the redox reaction taking place between GOx and platinum electrode along with the use of biocompatible nafion membrane. Well aligned ZnO nanorods with high aspect ratio contribute to the best performance in terms of sensitivity for glucose detection. The low cost fabrication method, with the achieved

high sensor sensitivity, encourage further investment and research towards commercialization of such electrochemical glucose sensors.

APPENDIX

The comparison of the performance parameters of other peer reported glucose sensors based on other nanomaterials grown on different substrates has been presented in Table I.

Table I

Working electrode material	Sensitivity ($\mu A/cm^2 mM$)	Response time (s)	Detection limit (mM)	Linear range (mM)	Reference
ZnO nanotubes/Au	21.7	3	0.001	0.05 – 12	9
ZnO nanorods/Si/Ag	106.6	< 2	0.001	0.01 – 17.0	10
ZnO nanocomb/Au	15.33	< 10	0.02	0.02 – 4.5	11
ZnO nanorods/Au	23.1	< 5	0.01	0.01 – 3.45	12
ZnO nanotubes	30.85	< 6	0.01	0.01 – 4.2	13
ZnO inverse opal	22.5	_	_	0.01 – 18	14
ZnO nanowires	24.56	_	_	0.01 – 7	14
TiO_2 sol-gel film	7.2	< 6	0.07	0.07 – 15	15
C-ZnO nanowires/Ti	35.3	~ 5	0.001	0.01 – 1.6	16
CeO_2/Au	0.00287	< 5	0.012	2.8 – 22.2	17
ZnO nanorods/ITO	1151	< 3	0.089	0.01 – 1.6	This work

REFERENCES

1. World Health Organization, www.who.int/diabetes/wdd_2015/en/ (last seen on 11/16/2015).
2. Zhou, J., Xu, N. S. and Wang, Z. L, Dissolving Behavior and Stability of ZnO Wires in Biofluids: A Study on Biodegradability and Biocompatibility of ZnO Nanostructures, Adv. Mater. 18 (2006) 2432-2435.
3. Zhao, Z., Lei, W., Zhang, X., Wang, B., & Jiang, H. ZnO-Based Amperometric Enzyme Biosensors. Sensors (Basel, Switzerland), 10(2), (2010) 1216-1231.
4. Mein Jin Tan, Shu Zhong, Jun Li, Zhikuan Chen, and Wei Chen, Air-Stable Efficient Inverted Polymer Solar Cells Using Solution-Processed Nanocrystalline ZnO Interfacial Layer, ACS Applied Materials & Interfaces, 5 (11), (2013) 4696-4701.
5. Juan Zuow and Andreas Erbe, Optical and electronic properties of native zinc oxide films on polycrystalline Zn, Phys. Chem. Chem. Phys. 12 (2010), 11467-11476.
6. Ibupoto, Z.H.; Khun, K.; Eriksson, M.; AlSalhi, M.; Atif, M.; Ansari, A.; Willander, M. Hydrothermal Growth of Vertically Aligned ZnO Nanorods Using a Biocomposite Seed layer of ZnO Nanoparticles. Materials, 6, (2013) 3584-3597.
7. W. Putzbach and N. J. Ronkainen, Immobilization Techniques in the Fabrication of Nanomaterial-Based Electrochemical Biosensors: A Review, Sensors 13, (2013) 4811-4840.

8. D. Wilke, H. Müller and N. Kolytsheva, Activated platinum electrodes as transducer for a glucose sensor using glucose oxidase in a photopolymer membrane, Fresenius J Anal Chem, 357, (1997) 534–538.
9. Tao Kong, Yang Chen, Yiping Ye, Kun Zhang, Zhenxing Wang, and Xiaoping Wang, An amperometric glucose biosensor based on the immobilization of glucose oxidase on the ZnO nanotubes, Sensors and Actuators B, 138, (2009) 344-350.
10. R. Ahmad, N. Tripathy, J. H. Kim and Y. Hahn, Highly selective wide linear-range detecting glucose biosensors based on aspect-ratio controlled ZnO nanorods directly grown on electrodes, Sensors & Actuators B. Chemical, 174, (2012) 195-201.
11. J. X. Wang, X.W. Sun, A. Wei, Y. Lei, X. P. Cai, C. M. Li and Z. L. Dong, Zinc oxide nanocomb biosensor for glucose detection, Applied Physics Letters, 88, (2006) 233106.
12. A. Wei, X. W. Sun, J. X. Wang, Y. Lei, X. P. Cai, C. M. Li, Z. L. Dong and W. Huang, Enzymatic glucose biosensor based on ZnO nanorod array grown by hydrothermal decomposition, Applied Physics Letters, 89, (2006) 123902.
13. Kun Yang, Guang-Wei She, Hui Wang, Xue-Mei Ou, Xiao-Hong Zhang, Chun-Sing Lee and Shuit-Tong Lee, ZnO Nanotube Arrays as Biosensors for Glucose, The Journal of Physical Chemistry C, 113, (2009) 20169-20172.
14. Xueqiu You, James H. Pikul, William P. King and James J. Pak., Zinc oxide inverse opal enzymatic biosensor, Appl. Phys. Lett., 102, (2013) 253103.
15. Jiuhong Yu, Songqin Liu and Huangxian Ju, Glucose sensor for flow injection analysis of serum glucose based on immobilization of glucose oxidase in titania sol–gel membrane, Biosensors and Bioelectronics, 19, (2003) 401-409.
16. J. Liu, C. Guo, C. M. Li, Y. Li, Q. Chi, X. Huang, L. Liao, and T. Yu, Carbon-decorated ZnO nanowire array: A novel platform for direct electrochemistry of enzymes and biosensing applications, Electrochemistry Communications, 11, (2009) 202-205.
17. A. A. Ansari, P. R. Solanki and B. D. Malhotra, Sol-gel derived nanostructured cerium oxide film for glucose sensor, Applied Physics Letters, 92, (2008) 263901.
18. L. Guo, S. Yang, C. Yang, P. Yu, J. Wang, W. Ge and G. K. L. Wong, Highly monodisperse polymer-capped ZnO nanoparticles, Preparation and optical properties, Appl. Phys. Lett., 76, (2000) 2901-2903.
19. Gu, Y. and Kuskovsky, Igor L. and Yin, M. and O'Brien, S. and Neumark, G. F., Quantum confinement in ZnO nanorods, Applied Physics Letters, 85, (2004) 3833-3835.
20. An-Jen Cheng, Yonhua Tzeng, Hui Xu, Siddharth Alur, Yaqi Wang, Minseo Park, Tsung-hsueh Wu, Curtis Shannon, Dong-Joo Kim and Dake Wang, Raman analysis of longitudinal optical phonon-plasmon coupled modes of aligned ZnO nanorods, Journal of applied physics 105 (2009) 073104.
21. Julia W. P. Hsu, Zhengrong R. Tian,Neil C. Simmons,Carolyn M. Matzke,James A. Voigt, and, Jun Liu, Directed Spatial Organization of Zinc Oxide Nanorods, Nano Letters, 5 (1), (2005) 83-86.
22. A. Monshi, M. F. Foroughi, and M. R. Monshi, Modified Scherrer Equation to Estimate More Accurately Nano-Crystallite Size Using XRD, World Journal of Nanoscience and Engineering 2 (2012) 154-160.
23. Armbruster, David A, and Terry Pry, Limit of Blank, Limit of Detection and Limit of Quantitation, The Clinical Biochemist Reviews 29.Suppl 1, (2008) S49–S52.
24. Shrivastava A and Gupta VB, Methods for the determination of limit of detection and limit of quantitation of the analytical methods, Chron Young Sci. 2 (2011) 21-25.